Research Square

Preprints are preliminary reports that have not undergone peer review.
They should not be considered conclusive, used to inform clinical practice,
or referenced by the media as validated information.

Comparison of the effects of the Invisalign Palatal Expander and an acrylic-bonded expansion appliance on craniofacial structures using finite element analysis

Zeynep Betül Yavuz

231114018@st.biruni.edu.tr

Biruni University

Esra Ağaoğlu Mogul

Biruni University

Research Article

Keywords: Invisalign Palatal Expander, Acrylic-bonded expansion appliance, Rapid maxillary expansion, Finite element analysis, Biomechanics, Midpalatal suture, Mixed dentition, Transverse maxillary deficiency

Posted Date: November 25th, 2026

DOI: https://doi.org/10.21203/rs.3.rs-11471471/v1

License: This work is licensed under a Creative Commons Attribution 4.0 International License.
Read Full License

Additional Declarations: No competing interests reported.

Comparison of the effects of the Invisalign Palatal Expander and an acrylic-bonded expansion appliance on craniofacial structures using finite element analysis

Zeynep Betül Yavuz[1]* and Esra Ağaoğlu Mogul[1]

[1] Department of Orthodontics, Faculty of Dentistry, Biruni University, Istanbul, Türkiye

* Corresponding author: Zeynep Betül Yavuz, Department of Orthodontics, Faculty of Dentistry, Biruni University, Merkezefendi Mah., G/75. Sok. No: 13B, 34015 Zeytinburnu, Istanbul, Türkiye. E-mail: 231114018@st.biruni.edu.tr

Email addresses: ZBY: 231114018@st.biruni.edu.tr; EAM: emogul@biruni.edu.tr

Abstract

Background: The Invisalign Palatal Expander (IPE) has recently emerged as an alternative to conventional rapid maxillary expansion appliances in growing patients, but evidence on its biomechanical behavior remains limited. This study compared the biomechanical responses produced by the IPE and a conventional acrylic-bonded expansion appliance (ABEA).

Methods: A patient-specific 3-dimensional finite element model of the craniofacial complex was reconstructed from cone-beam computed tomography data of a patient aged 8-10 years in the mixed dentition with maxillary transverse deficiency. Both appliances were analyzed under identical boundary and loading conditions, with a total prescribed transverse expansion of 10 mm (5 mm per side). Displacement and stress in the teeth, periodontal ligament, cortical bone, trabecular bone, and circummaxillary sutures were evaluated, together with opening of the midpalatal suture.

Results: Both appliances produced transverse expansion, but the responses differed. The ABEA produced greater total tooth displacement (4.533 vs 2.497 mm), cortical bone and sutural displacement (4.617 vs 2.119 mm), and trabecular bone displacement (3.378 vs 1.564 mm). Periodontal ligament stress was also higher with the ABEA (3.957 vs 2.238 MPa). Peak dental von Mises stresses were comparable (75.787 vs 74.899 MPa), but the ABEA showed broader stress propagation, whereas the IPE showed more localized transmission with lower magnitudes. The midpalatal suture opened in both models, in a wedge-shaped pattern wider anteriorly than posteriorly, and the opening was greater with the ABEA (5.570 mm anteriorly and 4.100 mm posteriorly) than with the IPE (2.414 and 1.928 mm, respectively).

Conclusions: Both systems achieved a similar overall expansion pattern but differed biomechanically. The ABEA produced more extensive displacement and stress transmission, whereas the IPE produced a more controlled response. These differences reflect force transmission under the simulated conditions rather than clinical superiority of either appliance.

Keywords: Invisalign Palatal Expander, Acrylic-bonded expansion appliance, Rapid maxillary expansion, Finite element analysis, Biomechanics, Midpalatal suture, Mixed dentition, Transverse maxillary deficiency

Background

Maxillary transverse deficiency is a common dentoskeletal problem observed during the mixed dentition and is frequently accompanied by posterior crossbite, dental crowding, functional mandibular deviation, and compromised occlusal relationships [1, 2]. If left untreated during growth, this discrepancy may adversely affect transverse arch development and overall craniofacial growth. Early diagnosis and appropriate intervention are therefore important for establishing normal maxillary width, improving occlusal function, and facilitating harmonious craniofacial development [1].

Rapid maxillary expansion (RME) is widely accepted as the standard orthopedic approach for correcting transverse maxillary deficiency in growing patients. By separating the midpalatal suture and transmitting expansion forces to the surrounding maxillary structures, RME increases the transverse dimension of the maxilla and produces both skeletal and dentoalveolar changes [2, 3].

Conventional acrylic-bonded rapid maxillary expanders have long been among the most commonly used appliances for correcting transverse maxillary deficiency in growing patients because of their ability to produce effective orthopedic expansion [2, 3]. However, these appliances may also induce undesirable biomechanical effects, including buccal tipping of the anchorage teeth, increased stress within the periodontal ligament, deformation of the alveolar bone, and transmission of expansion forces to the circummaxillary sutures [4, 5]. Previous finite element studies have demonstrated that the biomechanical response to maxillary expansion is influenced by appliance design, structural rigidity, activation protocol, and force delivery characteristics [4, 6]. These characteristics determine how expansion forces are transferred to the dentoalveolar complex and surrounding craniofacial structures, thereby influencing both the skeletal and dentoalveolar outcomes of expansion. Understanding the biomechanical behavior of different expansion appliances is therefore essential for optimizing treatment outcomes while minimizing undesirable side effects.

Recently, the Invisalign Palatal Expander (IPE) has emerged as a treatment option for correcting transverse maxillary deficiency in growing patients. Unlike conventional rapid maxillary expansion appliances, the IPE is a directly 3-dimensionally printed device fabricated from polyamide-12 (PA-12; nylon 12), a semicrystalline thermoplastic polymer, which provides a different mode of force delivery during expansion [7]. Clinical evidence on aligner-based maxillary expansion in the mixed dentition has so far been derived largely from studies of the Invisalign First system, which reported increases in transverse dimensions together with improved esthetics, patient comfort, and ease of oral hygiene compared with conventional expansion appliances [8, 9]. These systems are mechanically distinct from the IPE, and evidence specific to the IPE remains scarce. To date it is limited mainly to a pilot study reporting skeletal and dentoalveolar changes in a small sample

spanning a wide age range (6-18 years), the findings of which should be interpreted cautiously given age-related variability in midpalatal suture maturation [10]. Despite its growing clinical use, information on the biomechanical response of the teeth, periodontal ligament, cortical bone, trabecular bone, and circummaxillary structures during treatment with the IPE remains limited. Previous finite element research has compared conventional rapid palatal expansion with aligner-based expansion [11], but the appliances evaluated in that study were clear aligners rather than the IPE. An in-vitro investigation has also compared the mechanical behavior of a clear aligner and a rapid palatal expander in the transverse plane [12], although that study neither used finite element analysis nor evaluated the IPE. More recently, Ding et al. [13] investigated the biomechanical behavior of the IPE with 3-dimensional finite element analysis, evaluating the effects of different appliance thicknesses and incremental expansion step sizes. Their analysis demonstrated that variations in appliance thickness and expansion step size influenced posterior tooth displacement, periodontal ligament stress, and the mechanical response of the midpalatal suture, indicating that IPE biomechanics depend strongly on appliance design and activation parameters. However, that study focused on variations within the IPE system rather than directly comparing the IPE with a conventional acrylic-bonded expansion appliance. A direct biomechanical comparison of these 2 mechanically distinct expansion systems under identical modeling and loading conditions therefore remains warranted.

Finite element analysis (FEA) is a well-established computational method for evaluating stress distribution and displacement patterns within craniofacial structures under mechanical loading [4-6, 14]. In orthodontics, FEA enables 3-dimensional assessment of the biomechanical response of the teeth, periodontal ligament, cortical and trabecular bone, and circummaxillary sutures during maxillary expansion, providing information that cannot be obtained directly through clinical or experimental investigations [4-6]. Although FEA has been widely used to investigate the biomechanics of conventional rapid maxillary expansion appliances, only one previous finite element study has evaluated the biomechanical behavior of the IPE itself [13]. The differences in force transmission, stress distribution, and displacement patterns produced by these 2 expansion systems have therefore not yet been fully clarified.

The aim of this study was to compare the biomechanical behavior of an acrylic-bonded expansion appliance (ABEA) and the IPE, 2 mechanically distinct expansion systems, under identical modeling and loading conditions, with a patient-specific 3-dimensional finite element model representing the mixed dentition. The specific objective was to establish how each appliance distributes a prescribed transverse expansion through the craniofacial complex, by quantifying stress and displacement in the teeth, periodontal ligament, cortical bone, trabecular bone, and circummaxillary sutures, together with opening of the midpalatal suture. The null hypothesis was that the 2 expansion appliances would exhibit comparable biomechanical responses under identical loading conditions.

Methods

This study was approved by the Scientific Research Ethics Committee of Biruni University, Istanbul, Türkiye (approval no. 2024-BİAEK/14-22, dated October 20, 2025) and was

conducted in accordance with the Declaration of Helsinki. Written informed consent for the use of the anonymized cone-beam computed tomography (CBCT) data for research purposes was obtained from the patient's legal guardian.

A CBCT dataset obtained from a patient aged 8-10 years in the mixed dentition, diagnosed with maxillary transverse deficiency, was used to construct a 3-dimensional finite element model of the craniofacial complex. The scan had been acquired for diagnostic purposes before the study with a CS 9600 cone-beam computed tomography unit (Carestream Dental, Atlanta, GA, USA), using the pediatric acquisition protocol routinely applied at the institution for patients of this age rather than an adult protocol. The CBCT data in Digital Imaging and Communications in Medicine (DICOM) format were imported into 3D Slicer software (version 5.6; open source, https://www.slicer.org) for image segmentation. Tooth and maxillary bone structures were segmented with a gray-value threshold range of 429.50 to 3193.04 and exported as stereolithography files. Because CBCT gray values are not standardized Hounsfield units and vary with the scanner and the acquisition settings, this range was established for the present dataset and verified visually against the corresponding axial, coronal, and sagittal sections rather than applied as an absolute calibrated threshold. Unwanted structures and imaging artifacts were removed with the Erase and Scissors tools, and surface smoothing was then applied to the segmented models to eliminate digitization irregularities without altering the underlying bone contour, before 3-dimensional reconstruction (Fig. 1). Regions of the craniofacial skeleton that extended beyond the CBCT field of view, including the superior orbital margins, were completed by anatomic extension of the segmented geometry so that force transmission to the circummaxillary structures could be represented within a continuous model; these extended regions lie outside the area of interest and were not used for quantitative evaluation.

The stereolithography models were subsequently imported into Rhinoceros 3D (Robert McNeel & Associates, Seattle, WA, USA) for reverse engineering and computer-aided design (CAD). A 1.5-mm-thick cortical bone layer was generated by applying an inward offset to the external surface of the maxillary bone, whereas the remaining internal volume was defined as trabecular bone; this thickness is consistent with values used in previous craniofacial finite element models of maxillary expansion [4-6]. Circummaxillary sutures were modeled with thicknesses of 0.80 mm for the midpalatal suture and 0.50 mm for the zygomaticomaxillary, frontomaxillary, and frontonasal sutures, in accordance with sutural thicknesses reported in previous craniofacial finite element models [4-6]. The dentition segmented from the CBCT dataset was positioned within the maxillary model. The periodontal ligament was modeled as a uniform 0.25-mm-thick layer surrounding the root surfaces and extending 1 mm apical to the cementoenamel junction. After surface adaptation and contact adjustment, the 3-dimensional finite element model was completed.

Appliance design

Two maxillary expansion appliances were designed for biomechanical comparison: an ABEA and the IPE. Both devices had been physically fabricated for the same patient from whom the CBCT data were obtained: the IPE was manufactured for the patient by the supplier, and the ABEA was subsequently fabricated to the same dimensions, so that the 2

appliances corresponded to the same dental arch. Each physical appliance was measured with a digital caliper at the thickest point of every anatomic region, and the recorded dimensions were used to reproduce the devices in Rhinoceros 3D (Fig. 2). For the ABEA, the acrylic body was designed with a uniform thickness of 2.50 mm and incorporated a stainless steel expansion screw 7.50 mm in width positioned along the midpalatal region; the overall transverse width of the appliance was 55.35 mm (Fig. 2G). For the IPE, the geometry of the first appliance of the series was reproduced. Material thickness varied according to the anatomic region, measuring 1.20 mm on the buccal surfaces, 1.50 mm on the palatal surfaces, and 4.50 to 5.00 mm within the palatal expansion region (Fig. 2H). The appliance was modeled with the tapering thickness of the original device rather than with a uniform thickness within each region, and the values reported represent the maximum thickness recorded in each region. Both appliance models were positioned on the same 3-dimensional maxillary model and analyzed under identical loading and boundary conditions to enable direct biomechanical comparison.

Material properties

All materials were assumed to be homogeneous, isotropic, and linearly elastic, a commonly accepted assumption in craniofacial finite element analyses [4-6]. The mechanical properties of the craniofacial structures and conventional appliance components were assigned from values reported in previous finite element studies [4-6]. The IPE was modeled with polyamide-12 (PA-12; nylon 12), in accordance with the manufacturer's product information, which specifies that the appliance is a directly 3-dimensionally printed device fabricated from polyamide-12 [7]. An elastic modulus of 1650 MPa was assigned to PA12 on the basis of previously reported mechanical data for additively manufactured PA-12 [15], whereas a Poisson ratio of 0.40 was adopted in accordance with a recent finite element model of the IPE [13]. A Young modulus of 69 MPa was assigned to the periodontal ligament. Reported values for this tissue vary widely, from 0.01 to 175 MPa, and values of 68.9-69 MPa have been used in more than half of published dental finite element analyses [16]; the influence of this choice is addressed in the limitations. The material properties are summarized (Table 1).

Mesh generation and convergence analysis

The 3-dimensional geometric models were imported into HyperMesh (Altair Engineering, Troy, MI, USA) for finite element meshing. Surface meshes were initially generated with triangular shell elements, after which volumetric meshes were created with 4-node tetrahedral solid elements to ensure accurate geometric representation and numerical stability. Triangular 2-dimensional and tetrahedral 3-dimensional elements were used because they reproduce complex geometries and curved surfaces more faithfully, which is advantageous for organic structures such as bone. Mesh quality was verified in all models: triangles with a skewness greater than 80° and elements with a minimum edge length below 0.001 mm were identified and corrected before the analyses. A graded mesh was used. An element edge length of 0.1 mm was applied to the regions of interest, comprising the appliances, the dentition, the periodontal ligament, and the circummaxillary sutures, to provide sufficiently fine spatial discretization of these thin and mechanically critical

structures. In regions of larger volume remote from the area of interest, the element edge length was increased progressively to a maximum of 0.25 mm to maintain computational feasibility. The same meshing strategy was applied to both appliance models to ensure comparability (Fig. 3D). The final meshes, adopted after the convergence analysis described below, consisted of 737,602 nodes and 2,796,066 elements for the ABEA model and 649,830 nodes and 2,458,729 elements for the IPE model (Table 2). The completed models were exported to OptiStruct (Altair Engineering) for linear static finite element analysis.

A mesh convergence analysis was performed to confirm that the solution was independent of mesh density. A series of meshes with element edge lengths ranging from 0.4 to 0.1 mm was generated and analyzed under identical loading and boundary conditions. The analysis was performed on the ABEA model, which produced the higher stress and displacement magnitudes of the 2 models and therefore represented the more demanding case for spatial discretization; the mesh density established in this way was then applied unchanged to the IPE model. The peak maximum principal stress in the cortical bone was used as the convergence metric because it was the variable most sensitive to mesh refinement and therefore the most conservative basis on which to establish mesh independence. The relative error between successive meshes was calculated as the difference between the current and the preceding value, divided by the current value, expressed as a percentage. The relative error fell below the predefined threshold of 3% at an element edge length of 0.15 mm and decreased further to 0.96% at 0.1 mm, indicating that mesh independence had been achieved (Table 3). The 0.1-mm mesh was therefore adopted for all subsequent analyses.

Contact definitions

All interfaces between adjacent model components were defined with bonded (freeze) contact conditions to ensure numerical stability and consistent force transfer, an approach also adopted in previous finite element analyses of maxillary expansion appliances [17], so that no relative sliding or separation was permitted at the defined interfaces. The circummaxillary sutures were modeled as continuous soft-tissue volumes with the assigned sutural material properties (Table 1), and their interfaces with the adjacent bone were defined as bonded because a suture and the bone it joins form an anatomically continuous unit in which deformation and failure occur within the sutural tissue itself rather than by debonding at the sutural margin. The mechanical response of each suture was therefore represented by elastic deformation of the assigned sutural material.

Attachments were not modeled as separate geometric entities. Instead, the interface between the IPE and the tooth surfaces was defined as bonded, as a simplified representation of the attachment-mediated retention used clinically. The palatal mucosa was not included in the model, and consequently no contact was defined between the appliance and the palatal vault; in the absence of a mucosal layer, such contact would have been reduced to a direct appliance-bone interface and would have overestimated the stiffness of load transfer. Load was therefore transmitted to the craniofacial complex through the dentition alone, which is consistent with the clinical design of the IPE, a device that engages the teeth rather than the palatal mucosa. The same bonded interface

definition was retained in both models so that the comparison would reflect differences in appliance design rather than differences in contact formulation.

Boundary conditions and loading protocol

Transverse expansion was simulated by prescribing a displacement of 5 mm per side along the transverse (x) axis, corresponding to a total transverse expansion of 10 mm, applied identically to both appliance models (Fig. 3B, C). This prescribed displacement was selected to enable a standardized biomechanical comparison of the 2 appliance systems under identical total expansion conditions; it represents cumulative simulated expansion rather than a single clinical activation step and was not intended to reproduce the sequential activation protocol used clinically with the IPE.

Because both the geometry and the loading of the model were symmetric about the midsagittal plane, a half model was analyzed. The nodes lying on the midsagittal (y-z) plane were restrained in the transverse direction (Ux = 0). This is the standard symmetry condition for a half model and reproduces the behavior of the corresponding full model, in which the midsagittal plane itself does not translate transversely. The condition does not prevent transverse separation of the midpalatal suture: the sutural tissue and the maxillary structures lateral to the plane remain free to displace transversely, so that the opening of the suture is obtained as twice the transverse displacement of the sutural region lateral to that plane. The nodes along the superior and posterior cut boundaries of the maxillary model, that is, the truncated surfaces at which the model was separated from the remainder of the craniofacial skeleton, were fully constrained in all 6 degrees of freedom. Apart from these constraints, no additional restraint was imposed on the palate, the dentoalveolar structures, or the circummaxillary sutures, which remained free to deform under the applied load.

Expansion was simulated as an enforced displacement rather than as an applied force. The prescribed displacement was applied symmetrically at the midline of the expansion element of each appliance, corresponding to the position at which the expansion screw of the ABEA and the palatal expansion region of the IPE act clinically, and was distributed over adjacent nodes rather than applied to a single node to minimize stress singularities. The analyses were solved as linear static problems: no frictional contact was defined, all interfaces were bonded, and all materials were linearly elastic, so that no source of material, contact, or geometric nonlinearity was present. Under identical loading and boundary conditions, linear static analyses were performed for both appliance models (Fig. 3A).

Statistical analysis

Because the finite element analyses were deterministic numerical simulations performed under predefined material properties, boundary conditions, and loading conditions, no inferential statistical analysis was applicable. Comparisons between the 2 models were based on the magnitude and distribution of the calculated stress and displacement values.

Outcome measures

The following variables were evaluated: resultant (magnitude) displacement, calculated from the vector sum of the x-, y-, and z-direction displacements; directional displacement along the x (buccopalatal), y (mesiodistal), and z (occlusogingival) axes; maximum principal stress (P1), representing tensile stress; minimum principal stress (P3), representing compressive stress; and von Mises stress, used to evaluate the overall mechanical stress intensity regardless of loading direction. In addition, transverse displacement was recorded at 4 points distributed along the anteroposterior extent of the midpalatal suture in both models. Because the nodes lying exactly on the midsagittal plane are restrained in the transverse direction by the symmetry condition, the displacement was read at the first unconstrained node immediately lateral to that plane at each of these 4 positions. The corresponding total sutural opening was calculated as twice the recorded value, in accordance with the half-model symmetry condition described above. Stress values were expressed in megapascals and displacement values in millimeters.

Results

Dental displacement and stress distribution

The maximum total tooth displacement was 4.533 mm in the ABEA model and 2.497 mm in the IPE model, corresponding to approximately 44.9% lower total dental displacement in the IPE model (Fig. 4A, B). Transverse (x-direction) tooth displacement reached 4.497 mm in the ABEA model and 2.473 mm in the IPE model, a reduction of approximately 45.0% (Fig. 4C, D). Displacement in the y-direction was 0.574 mm in the ABEA model and 0.302 mm in the IPE model, approximately 47.4% lower mesiodistal displacement (Fig. 4E, F). Displacement in the z (vertical) direction was 1.122 mm in the ABEA model and 0.673 mm in the IPE model, approximately 40% lower in the IPE model (Fig. 4G, H).

In both appliance systems, the greatest displacement was observed in the posterior anchorage teeth, particularly the maxillary first molars, whereas the anterior teeth showed lower displacement values. The distribution of maximum von Mises stress differed between the 2 models. The maximum von Mises stress was 75.787 MPa in the ABEA model and 74.899 MPa in the IPE model (Fig. 5A, B). Although peak values were similar, the ABEA model showed elevated stress over a broader area of the dentition, whereas the IPE model showed localized regions of increased stress.

Cortical bone and circummaxillary sutural displacement and stress distribution

The maximum resultant displacement within the cortical bone and circummaxillary sutures was 4.617 mm in the ABEA model and 2.119 mm in the IPE model, approximately 54.1% lower in the IPE model (Fig. 6A, B). The maximum principal stress reached 79.547 MPa in the ABEA model and 41.429 MPa in the IPE model, approximately 47.9% lower tensile stress in the IPE model (Fig. 6C, D). The minimum principal stress was -58.520 MPa in the ABEA model and -38.622 MPa in the IPE model, approximately 34% lower compressive stress in the IPE model (Fig. 6E, F).

In both appliance systems, maximum principal (tensile) stress was concentrated within the alveolar process and adjacent lateral maxillary structures, whereas minimum principal (compressive) stress was distributed throughout the maxillary body and zygomatic buttress region. Both tensile and compressive stress distributions were more extensive and of greater magnitude in the ABEA model. Displacement was greater in the anterior maxillary region than in the posterior region, indicating a nonuniform anteroposterior distribution of the transverse response.

Midpalatal sutural opening

Transverse displacement along the midpalatal suture was greater in the ABEA model than in the IPE model over its entire anteroposterior extent. In the ABEA model, the transverse displacement recorded alongside the suture decreased from 2.785 mm at the most anterior point to 2.700, 2.248, and 2.050 mm at successive posterior points, corresponding to a sutural opening of 5.570 mm anteriorly and 4.100 mm posteriorly. In the IPE model, the corresponding displacements were 1.207, 1.188, 0.997, and 0.964 mm, corresponding to a sutural opening of 2.414 mm anteriorly and 1.928 mm posteriorly (Fig. 7). Sutural opening in the IPE model was therefore approximately 56.7% lower anteriorly and 53.0% lower posteriorly than in the ABEA model, and the ABEA produced approximately 2.3 times the anterior and 2.1 times the posterior sutural opening of the IPE.

In both models the suture opened in a wedge-shaped pattern that was wider anteriorly than posteriorly. The anteroposterior differential in sutural opening was 1.470 mm in the ABEA model and 0.486 mm in the IPE model, indicating that the more rigid appliance produced not only a larger but also a more markedly triangular pattern of sutural opening.

Periodontal ligament stress distribution

The maximum von Mises stress within the periodontal ligament was 3.957 MPa in the ABEA model and 2.238 MPa in the IPE model, approximately 43% lower in the IPE model (Fig. 5C, D). In both appliance systems, the highest stress concentrations were observed in the periodontal ligament of the posterior anchorage teeth, predominantly along the cervical region of the roots. Compared with the IPE model, the ABEA model showed a broader distribution of high stress values across the posterior anchorage teeth, whereas the IPE model showed more localized stress concentrations. In both models, relatively low stress values were observed in the periodontal ligament surrounding the anterior teeth.

Trabecular bone displacement and stress distribution

The maximum resultant displacement within the trabecular bone was 3.378 mm in the ABEA model and 1.564 mm in the IPE model, approximately 53.7% lower in the IPE model (Fig. 5E, F). The maximum principal stress of the trabecular bone reached 14.785 MPa in the ABEA model and 11.844 MPa in the IPE model, approximately 19.9% lower tensile stress in the IPE model. The minimum principal stress was -13.748 MPa in the ABEA model and -9.960 MPa in the IPE model, approximately 27.6% lower compressive stress in the IPE model.

In both appliance systems, the greatest trabecular bone displacement was observed in the alveolar process and anterior maxillary region, decreasing gradually toward the superior aspect of the maxilla. Maximum principal stress was predominantly concentrated within the alveolar trabecular bone surrounding the dental roots, whereas minimum principal stress was distributed more broadly throughout the trabecular bone of the maxillary body. Compared with the IPE model, the ABEA model showed greater displacement and more extensive distributions of both tensile and compressive stress.

Discussion

This finite element study compared the biomechanical effects of an ABEA and the IPE on the teeth, periodontal ligament, cortical bone, trabecular bone, and circummaxillary sutures of the craniofacial complex. The ABEA generated greater displacement of the teeth, cortical bone, and trabecular bone, together with higher stress values in the periodontal ligament and surrounding skeletal structures, than the IPE. Although both appliances produced a similar overall pattern of maxillary expansion, the magnitude and distribution of stress and displacement differed between the 2 models. The null hypothesis was therefore rejected.

Greater cortical bone displacement was observed in the ABEA model. This is consistent with previous finite element studies reporting that conventional rapid maxillary expansion appliances generate substantial skeletal displacement and stress within the maxillary complex [4, 5]. The greater skeletal response in the ABEA model may be attributed to the higher rigidity of the acrylic body and stainless steel expansion screw, which facilitates more direct transmission of expansion forces to the surrounding skeletal structures. In contrast, the lower cortical bone displacement in the IPE model may be related to the lower stiffness of the PA-12 appliance, whose elastic modulus (1650 MPa) is approximately 31% lower than that of the acrylic body (2400 MPa) and 2 orders of magnitude lower than that of the stainless steel expansion screw (200,000 MPa) of the ABEA. Cone-beam computed tomography evidence that conventional rapid maxillary expansion produces clinically detectable skeletal expansion of the maxilla supports this interpretation for the conventional appliance [18]; that evidence predates the IPE and does not extend to the comparison between the 2 systems.

In addition to the skeletal response, the ABEA model produced greater tooth displacement and higher periodontal ligament stress. In both appliance systems, the highest periodontal ligament stresses were concentrated in the cervical and furcation regions of the posterior anchorage teeth, consistent with previous finite element studies showing that posterior anchorage teeth are subjected to substantial mechanical loading during maxillary expansion [4, 5]. The higher periodontal ligament stress in the ABEA model may be attributed to the greater rigidity of the appliance, which allows expansion forces to be transmitted more directly to the supporting dentoalveolar structures.

Previous finite element evidence comparing conventional rapid palatal expansion with aligner-based expansion has similarly demonstrated appliance-dependent differences in stress distribution and displacement patterns [11]. However, the clear aligners evaluated in

that study differed from the IPE investigated here; direct quantitative comparison between the studies is therefore not appropriate.

Greater displacement in the cortical bone and sutural regions was observed in the ABEA model, consistent with previous finite element studies demonstrating that rapid maxillary expansion displaces the maxillary complex and transmits mechanical effects to the surrounding craniofacial structures [4-6]. Clinical imaging studies have also demonstrated changes in the circummaxillary sutures after rapid maxillary expansion [19, 20]. The greater displacement in the ABEA model may again reflect the higher rigidity of the appliance.

The midpalatal suture opened in both models, and the anteriorly wider, triangular configuration reproduced here corresponds to the pattern documented radiographically and tomographically after conventional rapid maxillary expansion [18-20]. This agreement provides a measure of face validity for the model. Of the 10 mm of prescribed transverse expansion, approximately 56% was expressed as sutural opening anteriorly in the ABEA model, compared with approximately 24% in the IPE model. The remaining proportion was accommodated by deformation of the appliance and by dentoalveolar displacement and bending of the maxillary halves. This distinction is clinically relevant because it indicates that the 2 appliances differ not only in the magnitude of the response they generate but also in how the prescribed expansion is partitioned between skeletal and dentoalveolar components. The lower proportion of skeletal expression in the IPE model is consistent with the lower stiffness of the PA-12 appliance, a greater share of the prescribed displacement being absorbed by deformation of the device itself. Because sutural opening in a finite element model depends on the assigned sutural stiffness, which is itself subject to considerable uncertainty, these proportions should be compared between the 2 appliances rather than interpreted as absolute predictions of clinical sutural expansion.

Another relevant finding was the nonuniform anteroposterior pattern of the transverse response in both appliance models. Displacement was consistently greater anteriorly than posteriorly, producing a wedge-shaped rather than a uniform anteroposterior distribution. The sutural displacement data confirm that this pattern represented genuine triangular separation of the maxillary halves rather than bending alone: the midpalatal suture opened 5.570 mm anteriorly and 4.100 mm posteriorly in the ABEA model and 2.414 and 1.928 mm, respectively, in the IPE model. The pattern is consistent with the biomechanical constraints imposed by the surrounding craniofacial structures and with patterns previously reported in finite element investigations of rapid maxillary expansion [4-6]. Although the magnitude of displacement differed between the models, the similar overall pattern suggests that craniofacial anatomy and posterior skeletal resistance continue to influence the spatial distribution of expansion irrespective of appliance design.

Although both appliance systems achieved transverse expansion, the IPE model showed lower stress and displacement values in the dentoalveolar and skeletal structures under identical prescribed expansion conditions. This is consistent with the limited clinical evidence available for the IPE, which suggests that it increases maxillary transverse dimensions in growing patients [10]. The lower values in the IPE model may be related to the lower stiffness of the PA-12 appliance, which may allow a greater proportion of the

prescribed displacement to be accommodated by deformation of the appliance itself, thereby reducing mechanical load transmission to the supporting structures. The biomechanical differences between the 2 systems should therefore be interpreted as differences in force transmission under the simulated loading conditions rather than as evidence of superior clinical effectiveness.

A recent finite element study by Ding et al. [13] further demonstrated that the biomechanical response of the IPE is strongly influenced by appliance thickness and incremental expansion step size. Increasing IPE thickness resulted in greater buccal displacement of the posterior teeth, increased initial displacement of the midpalatal suture, and higher periodontal ligament stress, and expansion step size also affected the magnitude and distribution of the mechanical response. These findings support the present observation that the mechanical properties and stiffness of the PA-12 appliance play an important role in determining how expansion loads are transmitted. However, direct quantitative comparison between the 2 studies should be approached cautiously because Ding et al evaluated incremental expansion steps of 0.1-0.3 mm, whereas this study used a cumulative prescribed transverse displacement of 10 mm [13].

The ABEA model also showed greater trabecular bone displacement and principal stress. Trabecular bone, despite its lower elastic modulus compared with cortical bone, contributes to the transmission and distribution of expansion forces within the maxillary complex. The greater trabecular response in the ABEA model is consistent with the overall pattern of greater skeletal response with the more rigid conventional appliance and with previous finite element evidence demonstrating stress transmission throughout the supporting maxillary structures [4].

The simultaneous increase in dental and skeletal displacement in the ABEA model also warrants consideration. Greater skeletal displacement was accompanied by greater tooth displacement and periodontal ligament stress, indicating that the increased mechanical response was not confined to the skeletal structures. The greater displacement produced by the ABEA should therefore not be interpreted as evidence of a proportionally greater skeletal effect; rather, it indicates more extensive transmission of the prescribed displacement throughout both the dentoalveolar and skeletal components. Determining whether either appliance produces a more favorable ratio of skeletal to dentoalveolar expansion would require separate quantitative assessment of these components.

A strength of this study is the use of a patient-specific CBCT-based finite element model representing the mixed dentition. Both appliances had been physically fabricated for this same patient and were reconstructed from direct caliper measurement of the actual devices rather than from generic designs, and identical loading and boundary conditions were applied to both models, allowing a standardized direct comparison while maintaining the same underlying craniofacial anatomy and the same dental arch.

Several limitations should be acknowledged. First, the model was constructed from the CBCT data of a single patient, which may limit generalizability. That patient was in the mixed dentition, within the 8-10-year age range, and the midpalatal suture was modeled accordingly as a patent, unossified structure. The results therefore apply to patients at a

comparable stage of sutural maturation and should not be extrapolated to adolescents or adults, in whom progressive sutural interdigitation increases resistance to transverse expansion and would be expected to reduce the sutural opening obtained with either appliance. All materials were assumed to be homogeneous, isotropic, and linearly elastic, and biologic factors such as bone remodeling, sutural adaptation, and muscular forces were not incorporated. The pterygomaxillary and pterygopalatine region was not modeled as a separate sutural interface; because this region represents an important site of posterior resistance during maxillary expansion [14], its omission may have influenced the simulated posterior stress and displacement patterns. Furthermore, the 10-mm transverse displacement represented cumulative simulated expansion applied as a standardized loading condition and does not reproduce the sequential incremental activation protocol used clinically, particularly for the IPE. The relatively high peak stress values in some structures may also have been influenced by the magnitude of the prescribed displacement and by localized stress concentrations inherent to finite element modeling; absolute stress magnitudes should therefore be interpreted with caution, with greater emphasis on the relative differences between the 2 models. The Young modulus assigned to the periodontal ligament (69 MPa) lies within the range most frequently used in dental finite element analyses but at the stiffer end of the reported spectrum; values approximately 2 orders of magnitude lower, in the region of 0.7 MPa, have been adopted in some recent models of aligner-based expansion, reflecting the low-strain nonlinear behavior of the ligament rather than its apparent stiffness at higher strain. Because periodontal ligament stress is sensitive to this parameter, the absolute periodontal ligament stresses reported here should be regarded as model-dependent and compared between the 2 appliances rather than interpreted in absolute terms.

Further limitations concern the modeling assumptions. All interfaces were modeled with bonded contact, preventing relative sliding or separation between adjacent components. The bonded contact between the IPE and the teeth represents an idealized condition of complete appliance-tooth engagement and does not fully reproduce the clinical interface, where local sliding, incomplete contact, or disengagement may occur; attachments were not modeled as separate entities, and the bonded definition therefore represents attachment-mediated retention in simplified form and may overestimate the efficiency of load transfer from the IPE to the dentition. Recent finite element modeling of the IPE has incorporated nonbonded appliance-tooth contact conditions [13], highlighting the potential influence of contact assumptions on simulated force transmission. An identical bonded definition was nevertheless retained in both models, because the 2 appliances engage the dentition over markedly different contact areas and introducing a frictional formulation, for which no validated coefficient is available for either interface, would have confounded the effect of appliance design with the effect of the contact assumption. The sutural interfaces were likewise bonded, so that sutural opening was obtained as elastic deformation of the assigned sutural material and no criterion for sutural failure or disruption was incorporated; the computed sutural openings are consequently dependent on the assigned sutural modulus, for which reported values vary considerably.

The analyses were solved as linear static problems. The computed response therefore scales linearly with the prescribed displacement, and geometric nonlinearity associated

with the magnitude of the simulated expansion was not accounted for. The mesh convergence analysis was performed on the ABEA model alone and used a single peak stress value as its metric; peak values are more sensitive to local mesh refinement than field averages, so mesh independence was established conservatively but not verified separately for the IPE model. For the periodontal ligament, only von Mises stress was evaluated; maximum and minimum principal stresses would have distinguished tensile from compressive loading within this tissue more clearly and would be informative in future analyses. Finally, regions of the craniofacial skeleton lying beyond the CBCT field of view were completed by anatomic extension of the segmented geometry; although these regions lie outside the area of interest and were not evaluated quantitatively, they are not patient-specific. These findings should therefore be interpreted primarily as a relative biomechanical comparison of the 2 appliance systems under the prescribed simulation conditions rather than as direct predictions of clinical behavior during individual activation steps.

Conclusions

Within the limitations of this finite element study, both appliance systems produced transverse expansion of the maxillary complex under the prescribed simulation conditions. The ABEA generated greater displacement of the teeth, cortical bone, and trabecular bone, greater opening of the midpalatal suture, and higher stress values in the periodontal ligament and surrounding skeletal structures, whereas the IPE showed lower stress and displacement values while maintaining a similar overall expansion pattern, including the anteriorly wider, triangular configuration of sutural opening. These differences indicate distinct biomechanical responses and force-transmission characteristics between the 2 appliance systems under identical prescribed expansion conditions. The lower stress and displacement values observed with the IPE should be interpreted as differences in mechanical load transmission rather than as evidence of superior clinical effectiveness. Further clinical and biomechanical studies incorporating incremental activation protocols and more realistic appliance-tooth contact conditions are warranted.

List of abbreviations

ABEA: Acrylic-bonded expansion appliance; CAD: Computer-aided design; CBCT: Cone-beam computed tomography; DICOM: Digital Imaging and Communications in Medicine; DOF: Degrees of freedom; FEA: Finite element analysis; IPE: Invisalign Palatal Expander; MPa: Megapascal; P1: Maximum principal stress; P3: Minimum principal stress; PA-12: Polyamide-12; PDL: Periodontal ligament; RME: Rapid maxillary expansion; STL: Stereolithography.

Declarations

Ethics approval and consent to participate

The study protocol was approved by the Scientific Research Ethics Committee of Biruni University, Istanbul, Türkiye (approval no. 2024-BİAEK/14-22, dated October 20, 2025). The study was conducted in accordance with the Declaration of Helsinki. Written informed consent for the use of the anonymized CBCT data for research purposes was obtained from the patient's legal guardian.

Consent for publication

Not applicable.

Availability of data and materials

The datasets generated and analyzed during the current study are available from the corresponding author on reasonable request.

Competing interests

The authors declare that they have no competing interests. The finite element analyses were performed by Tinus Technologies (Istanbul, Türkiye) as a paid technical service commissioned by the first author. The company had no role in the design of the study, the interpretation of the results, or the decision to submit the manuscript for publication.

Funding

This research received no grant from any funding agency in the public, commercial, or not-for-profit sectors.

Authors' contributions

Z.B.Y. conceived and designed the study, selected the clinical case and provided the cone-beam computed tomography data, measured the physical appliances, interpreted the finite element results, prepared the figures and tables, and wrote the main manuscript text. E.A.M. contributed to the conception and design of the study, supervised the project, interpreted the results, and critically revised the manuscript for important intellectual content. Both authors reviewed and approved the final manuscript.

Acknowledgements

The authors thank the engineering analysis team at Tinus Technologies for the image segmentation, the computer-aided design of the appliance and craniofacial models, the mesh generation and the numerical analyses.

Use of generative artificial intelligence and AI-assisted technologies

During the preparation of this work the authors used a generative artificial intelligence assistant to help with language editing of the manuscript text and with editing of the figure panels. After using this tool, the authors reviewed and edited the content as needed and take full responsibility for the content of the published article.

References

1. McNamara JA Jr. Maxillary transverse deficiency. Am J Orthod Dentofacial Orthop. 2000;117:567–70.
2. Bishara SE, Staley RN. Maxillary expansion: clinical implications. Am J Orthod Dentofacial Orthop. 1987;91:3–14.
3. Haas AJ. Palatal expansion: just the beginning of dentofacial orthopedics. Am J Orthod. 1970;57:219–55.
4. Işeri H, Tekkaya AE, Öztan Ö, Bilgiç S. Biomechanical effects of rapid maxillary expansion on the craniofacial skeleton studied by the finite element method. Eur J Orthod. 1998;20:347–56.
5. Jafari A, Shetty KS, Kumar M. Study of stress distribution and displacement of various craniofacial structures following application of transverse orthopedic forces: a three-dimensional FEM study. Angle Orthod. 2003;73:12–20.
6. MacGinnis M, Chu H, Youssef G, Wu KW, Machado AW, Moon W. The effects of micro-implant assisted rapid palatal expansion (MARPE) on the nasomaxillary complex: a finite element method study. Prog Orthod. 2014;15:52. https://doi.org/10.1186/s40510-014-0052-y.
7. Align Technology. Invisalign Palatal Expander System: product information for doctors. https://www.invisalign.com/provider/invisalign-solutions/for-orthodontists/for-kids/invisalign-palatal-expander. Accessed 10 Aug 2026.
8. Bruni A, Ferrillo M, Gallo V, Parrini S, Garino F, Castroflorio T, et al. Efficacy of clear aligners vs rapid palatal expanders on palatal volume and surface area in mixed dentition patients: a randomized controlled trial. Am J Orthod Dentofacial Orthop. 2024;166:203–14.
9. Lu L, Zhang L, Li C, Yi F, Lei L, Lu Y. Treatment effects after maxillary expansion using Invisalign First system versus acrylic splint expander in mixed dentition: a prospective cohort study. BMC Oral Health. 2023;23:598. https://doi.org/10.1186/s12903-023-03312-4.
10. Levrini L, Saran S, Imbesi E, Vanini I, Russo V, Rimoldi V, et al. Skeletal and dentoalveolar effects on the midpalatal suture and maxillary arch assessed by occlusal radiographs and three-dimensional digital models in patients treated with Invisalign palatal expander and rapid palatal expander: a pilot study. Front Dent Med. 2026;7:1757094. https://doi.org/10.3389/fdmed.2026.1757094.
11. Kurnaz M, Dayan E. Comparison of the effects of maxillary expansion applying rapid palatal expanders or clear aligners in mixed dentition: a three-dimensional finite

element study. J Orofac Orthop. 2025. https://doi.org/10.1007/s00056-025-00590-1.
12. Bruni A, Abate A, Maspero C, Castroflorio T. Comparison of mechanical behavior of clear aligner and rapid palatal expander on the transverse plane: an in vitro study. Bioengineering (Basel). 2024;11:103.
13. Ding L, Hui J, Qiao H. Effects of different aligner thicknesses and expansion step sizes on maxillary arch expansion with Invisalign Palatal Expander: a three-dimensional finite element study. BMC Oral Health. 2026. https://doi.org/10.1186/s12903-026-09033-8.
14. Holberg C, Steinhäuser S, Rudzki-Janson I. Rapid maxillary expansion in adults: cranial stress reduction depending on the extent of surgery. Eur J Orthod. 2007;29:31–6.
15. Kozior T, Hanon MM, Zmarzły P, Gogolewski D, Rudnik M, Szot W. Evaluation of the influence of technological parameters of selected 3D printing technologies on tribological properties. 3D Print Addit Manuf. 2024;11:e1567–80.
16. Celik HK, Koc S, Kustarci A, Rennie AEW. A literature review on the linear elastic material properties assigned in finite element analyses in dental research. Mater Today Commun. 2022;30:103087. https://doi.org/10.1016/j.mtcomm.2021.103087.
17. Ouldyerou A, Mamboleo E, Gilchrist L, Alsharif K, Ngan P, Merdji A, et al. In-silico evaluation of orthodontic miniscrew-assisted rapid palatal expanders for patients with various stages of skeletal maturation. Am J Orthod Dentofacial Orthop. 2024;166:561–71. https://doi.org/10.1016/j.ajodo.2024.07.018.
18. Garrett BJ, Caruso JM, Rungcharassaeng K, Farrage JR, Kim JS, Taylor GD. Skeletal effects to the maxilla after rapid maxillary expansion assessed with cone-beam computed tomography. Am J Orthod Dentofacial Orthop. 2008;134:8.e1–11.
19. Ghoneima A, Abdel-Fattah E, Hartsfield JK Jr, El-Bedwehi A, Kamel A, Kula K. Effects of rapid maxillary expansion on the cranial and circummaxillary sutures. Am J Orthod Dentofacial Orthop. 2011;140:510–9.
20. Leonardi R, Sicurezza E, Cutrera A, Barbato E. Early post-treatment changes of circumaxillary sutures in young patients treated with rapid maxillary expansion. Angle Orthod. 2011;81:36–41.

Figure legends

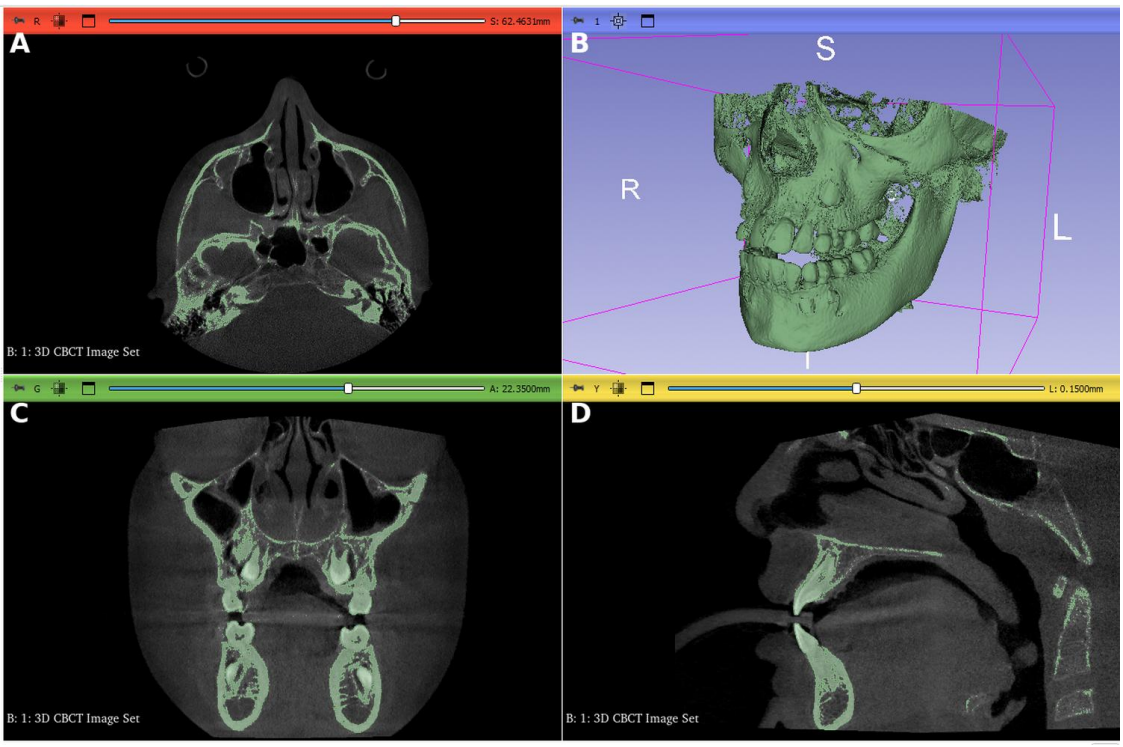

Fig. 1 Cone-beam computed tomography segmentation and 3-dimensional reconstruction of the craniofacial model. **A** axial section, **B** 3-dimensional reconstruction, **C** coronal section, **D** sagittal section

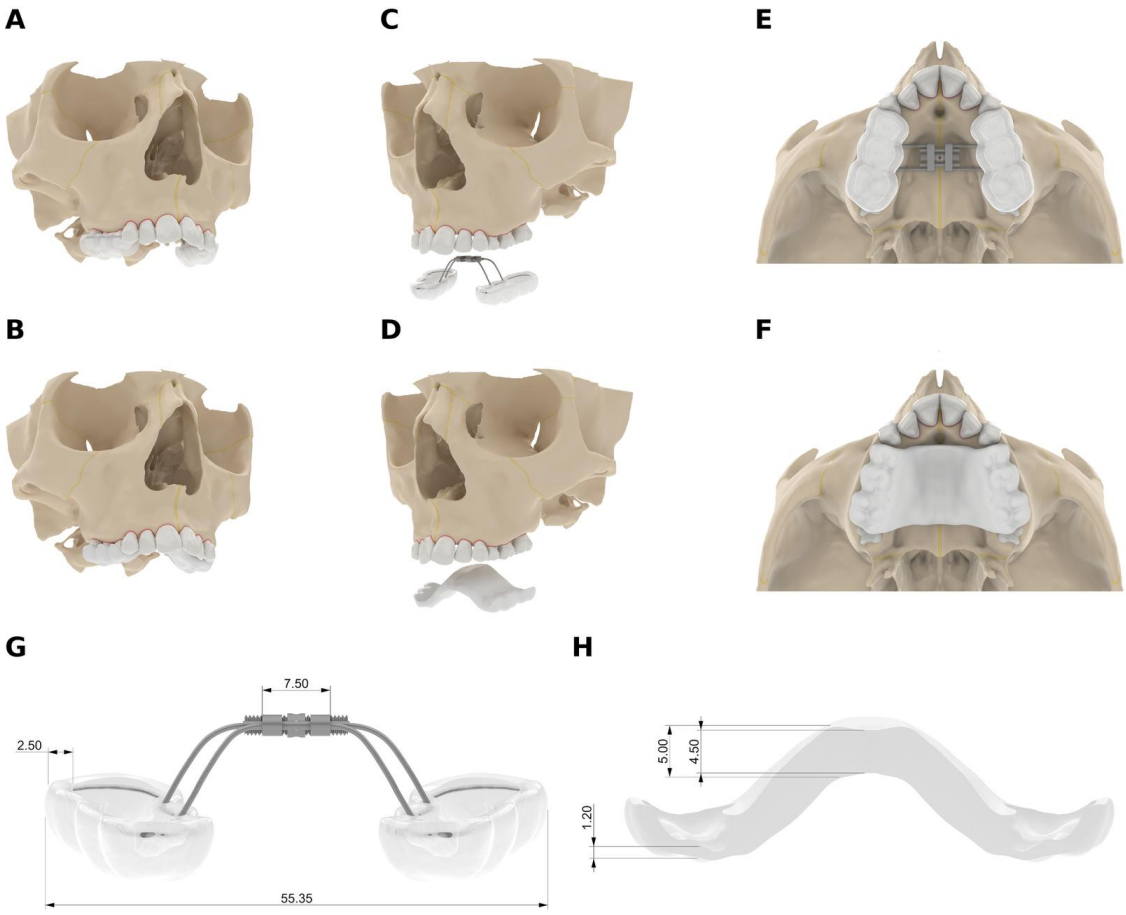

Fig. 2 Design and positioning of the 2 expansion appliances. **A** acrylic-bonded expansion appliance positioned on the maxillary model, **B** Invisalign Palatal Expander positioned on the maxillary model, **C** exploded view of the acrylic-bonded expansion appliance, **D** exploded view of the Invisalign Palatal Expander, **E** occlusal view of the acrylic-bonded expansion appliance, **F** occlusal view of the Invisalign Palatal Expander, **G** computer-aided design dimensions of the acrylic-bonded expansion appliance, **H** computer-aided design dimensions of the Invisalign Palatal Expander. All dimensions are given in millimeters

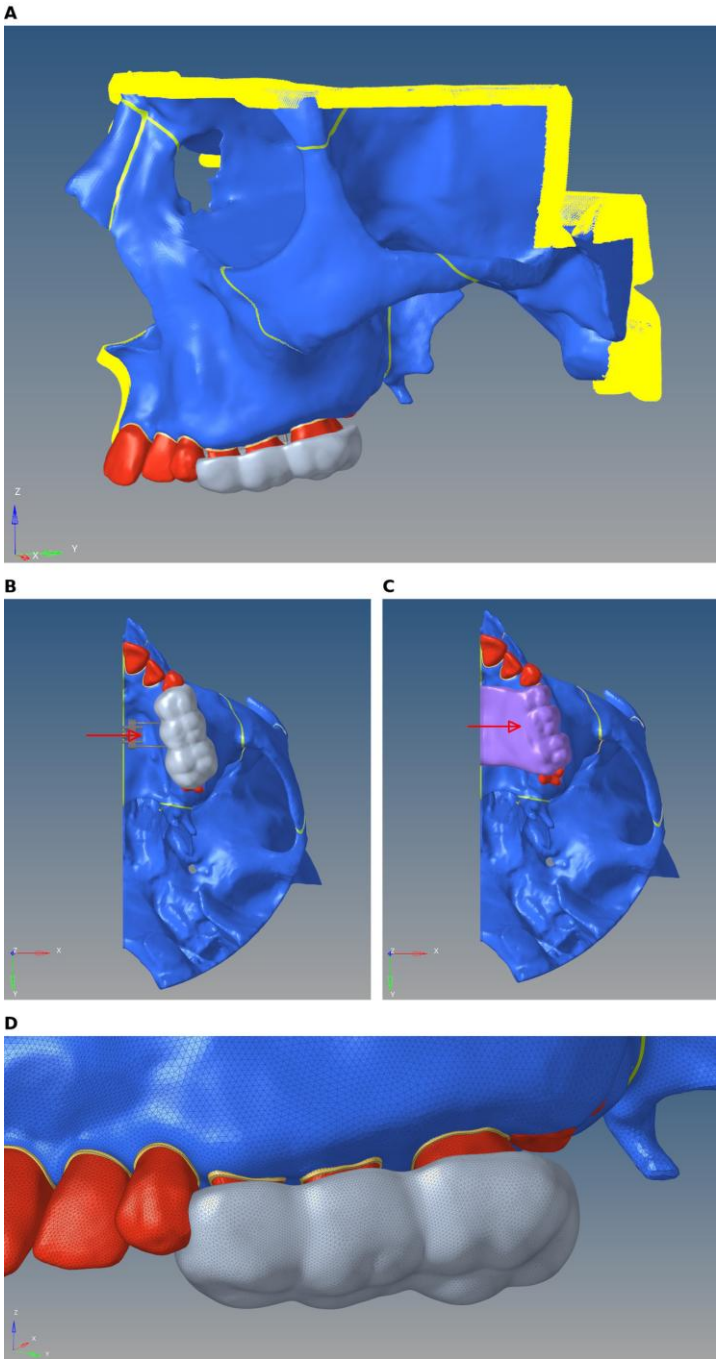

Fig. 3 Finite element model setup and simulation conditions. **A** boundary fixation conditions applied to the maxillary model, with the constrained nodes shown in yellow, **B** prescribed transverse displacement applied to the acrylic-bonded expansion appliance model, **C** prescribed transverse displacement applied to the Invisalign Palatal Expander model, **D** finite element mesh of the patient-specific maxillary model

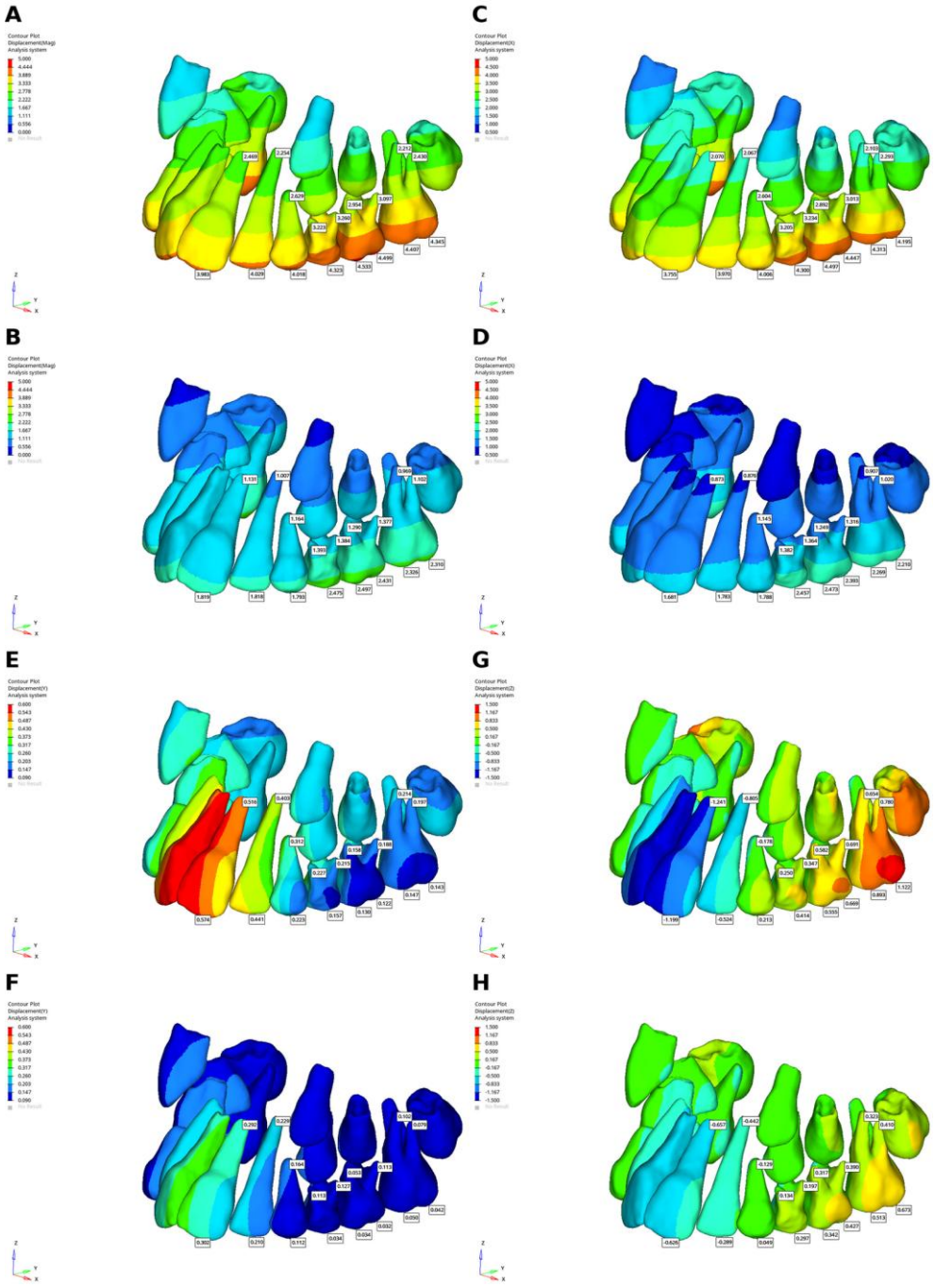

Fig. 4 Tooth displacement. **A** total displacement, acrylic-bonded expansion appliance (ABEA), **B** total displacement, Invisalign Palatal Expander (IPE), **C** x-direction displacement, ABEA, **D** x-direction displacement, IPE, **E** y-direction displacement, ABEA, **F** y-direction displacement, IPE, **G** z-direction displacement, ABEA, **H** z-direction displacement, IPE

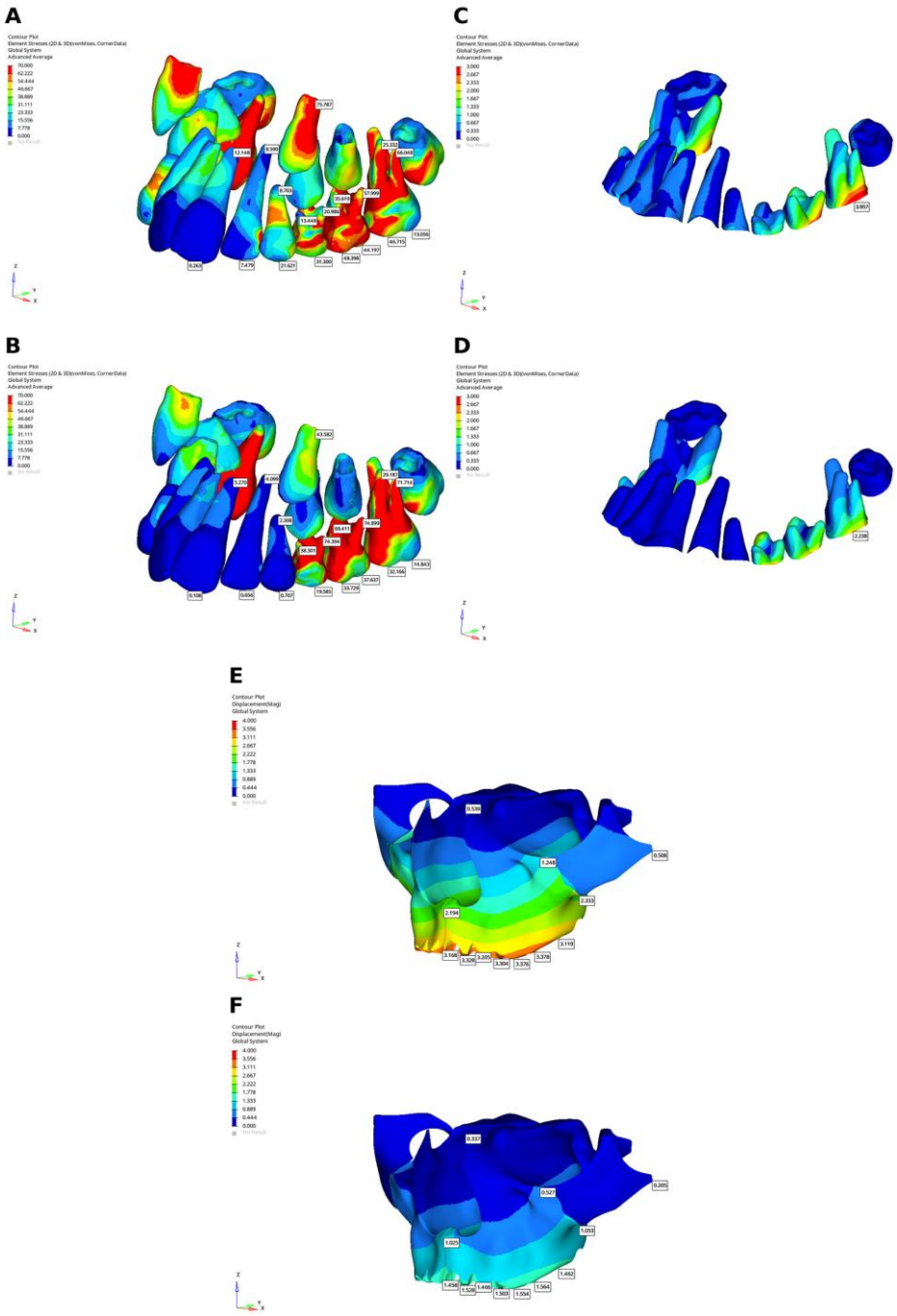

Fig. 5 Stress in the dentoalveolar structures and displacement of the trabecular bone. **A** dental von Mises stress, ABEA, **B** dental von Mises stress, IPE, **C** periodontal ligament von Mises stress, ABEA, **D** periodontal ligament von Mises stress, IPE, **E** trabecular bone displacement, ABEA, **F** trabecular bone displacement, IPE

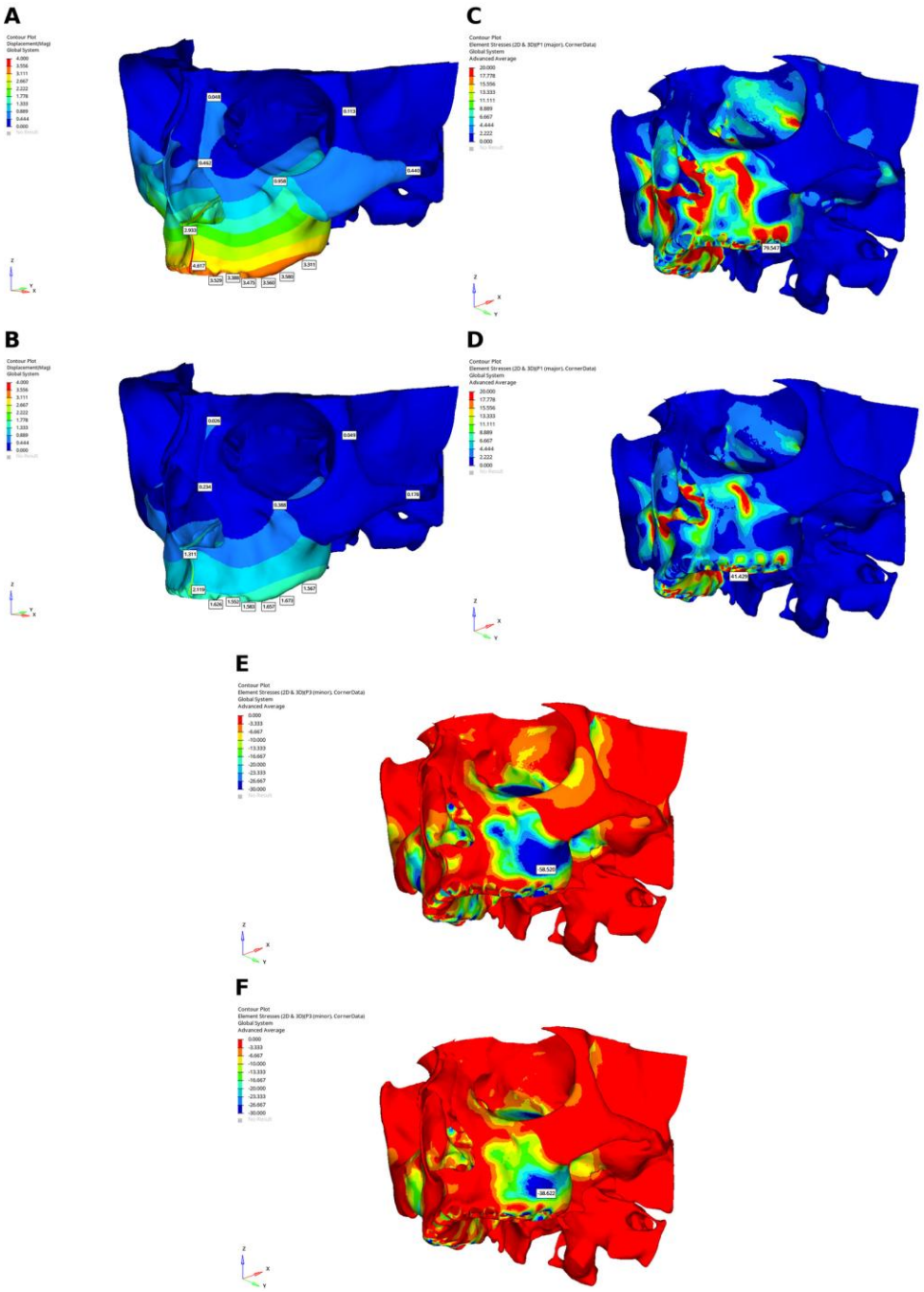

Fig. 6 Displacement and stress in the cortical bone and circummaxillary sutures. **A** resultant displacement, ABEA, **B** resultant displacement, IPE, **C** maximum principal stress, ABEA, **D** maximum principal stress, IPE, **E** minimum principal stress, ABEA, **F** minimum principal stress, IPE

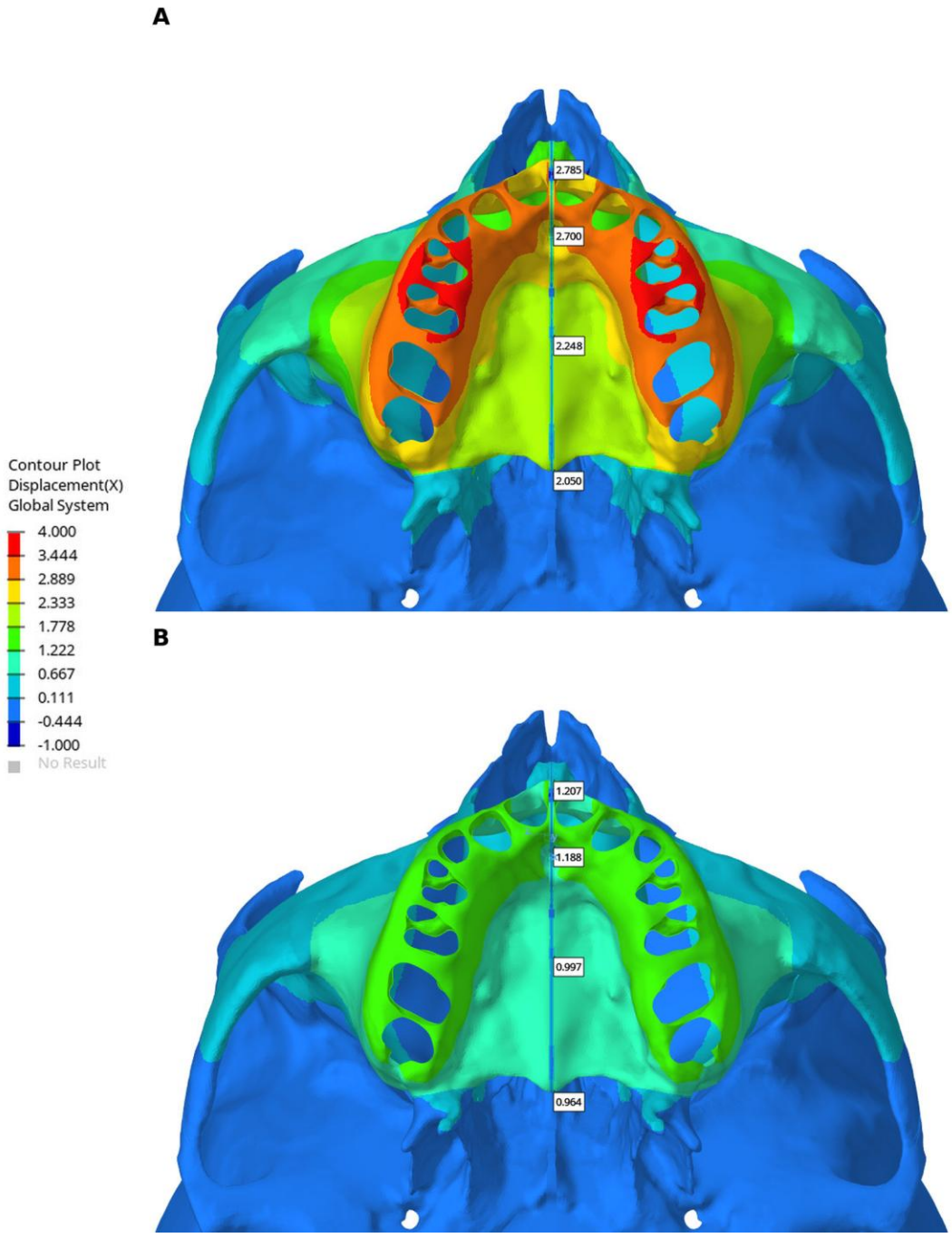

Fig. 7 Transverse (x-direction) displacement of the midpalatal suture, shown on the occlusal view of the maxillary complex, with values recorded at 4 points along its anteroposterior extent. **A** ABEA, **B** IPE. Values are the transverse displacement recorded at the first unconstrained node lateral to the midsagittal plane in the half model; the corresponding total sutural opening is twice the value shown

Tables

Table 1 Mechanical properties assigned to the finite element models

Material	Young modulus (MPa)	Poisson ratio
Cortical bone	14,500	0.30
Trabecular bone	1500	0.30
Teeth	18,600	0.31
Periodontal ligament	69	0.45
Acrylic	2400	0.30
Polyamide-12 (PA-12; nylon 12)	1650	0.40
Stainless steel	200,000	0.30
Sutures	0.68	0.45

The Young modulus assigned to the periodontal ligament (69 MPa) is the value most frequently used in dental finite element analyses [16]; its selection and the sensitivity of periodontal ligament stress to this parameter are addressed in the Methods and in the limitations

Table 2 Total numbers of nodes and elements used in the finite element models

Model	Total nodes	Total elements
ABEA model	737,602	2,796,066
IPE model	649,830	2,458,729

ABEA acrylic-bonded expansion appliance, *IPE* Invisalign Palatal Expander

Table 3 Mesh convergence analysis showing the peak maximum principal stress in the cortical bone of the ABEA model and the relative error between successive mesh refinements

Element edge length in the regions of interest (mm)	Maximum principal stress (MPa)	Relative error (%)
0.4	70.903	—
0.3	75.129	5.62
0.2	77.730	3.35
0.15	78.787	1.34
0.1	79.547	0.96

ABEA acrylic-bonded expansion appliance